PHYSICAL REVIEW B VOLUME 47, NUMBER 11 15 MARCH 1993-I

Model of self-trapped excitons in alkali halides

V. E. Puchin, A. L. Shluger, K. Tanimura, and N. Itoh
Department of Physics, Faculty of Science, Nagoya University, Furocho, Nagoya 464-01, Japan

(Received 27 July 1992)

We have carried out an *ab initio* many-electron variational calculation of the adiabatic potential-energy surface (APES) for the lowest triplet state of the self-trapped exciton (STE) in LiCl, NaCl, and KCl. Calculations of the *H* center in these crystals show that the ⟨111⟩ orientation is favored, in agreement with experimental results for NaCl but not for KCl, in which it is oriented along a ⟨110⟩ direction (no measurement exists for LiCl), and hence most detailed calculations for STE's are carried out for NaCl. It is found that the APES minimum for each crystal occurs when the Cl_2^- molecular ion is displaced along its molecular axis from its symmetrical position (D_{2h}) nearly halfway to the nearest halogen lattice point. The calculated transition energies for the optical absorption and luminescence at this configuration agree with the experimental values for the triplet STE, although the calculated stretching vibration frequency of the Cl_2^- molecular ion in NaCl is much smaller than that for the *H* center, contradictory to recent resonant Raman studies. Other minima are found at the nearest *F*-*H* pair configuration, in which the Cl_2^- molecular ion is reoriented by 90° from the initial orientation and next-nearest *F*-*H* pair. Extremely small luminescence energy at these configurations excludes the possibility that they are the candidates for the luminescent state of the STE. It is found that, after the displacement of the Cl_2^- molecular ion beyond the first minimum of the APES towards the nearest *F*-*H* pair configuration, the total energy is lowered by reorientation, inducing an anomaly on the APES. The results of a recent experimental investigation, including existence of several types of relaxed configuration of the STE in alkali halides, the stretching vibration frequency, and the femtosecond oscillation on APES, are discussed on the basis of the results of the calculation.

I. INTRODUCTION

The self-trapping of excitons has been observed in a wide variety of insulating solids with strong exciton-lattice coupling, such as alkali halides, alkaline earth fluorides, and some oxides.[1,2] This phenomenon is known to be responsible for various radiation-induced processes in the bulk[3,4] and on the surfaces of solids.[5] In particular, defect formation in the bulk and particle emission from the surface have been studied extensively and, indeed, correlated with the self-trapping of excitons. Very recently, the importance of the self-trapping of excitons in the mechanisms of radiation-induced processes in technologically important materials, such as silicon dioxide and alkaline earth halides, have been demonstrated.[2] The alkali halides are traditionally regarded as prototype materials in which the microscopic features of self-trapping processes have been studied most extensively. Despite the simplicity of the crystal structure and abundant knowledge of properties of radiation-induced processes, the mechanisms of self-trapping and the models of excitons in these crystals are not understood satisfactorily.

As has been established using electron-spin-resonance techniques,[6,7] the self-trapped excitons (STE's) in alkali halides consist of a hole, relaxed to the form of a X_2^- molecular ion (X denotes a halogen atom) and an electron. More elaborate experimental studies to elucidate the electronic and atomic structures of the STE have been carried out during the last few decades, using optical absorption,[8] luminescence,[1,2] electron-nuclear double resonance (ENDOR),[9] dynamics of formation in picosecond and femtosecond ranges,[10–12] resonant Raman scattering (RRS),[13] and other techniques.[2]

Several attempts have been made recently to classify the luminescent states of the STE in various alkali halides. Analyzing the STE luminescence of pure and mixed alkali halides of the NaCl structure, Kan'no, Tanaka, and Hayashi[14] categorized three types of luminescent states: types I, II, and III. Similar categorization has been made on the basis of the Mollwo-Ivey plots of the optical-absorption energies from the luminescent state as a function of lattice constant.[15] Since each luminescent state corresponds to a minimum of the adiabatic potential-energy surface (APES) of the lowest state of the STE, the capability of classifying into three groups suggested that the APES of alkali halides should have minima of different characters; type I appears in all alkali halides except in KCl and RbCl, while either type II or type III appears in most alkali halides. Existence of all three minima has been shown only in RbI (Refs. 16 and 17) and NaCl.[12] In the latter, an anticorrelated dumped oscillation of the heights of two optical-absorption bands after excitation of the lowest STE to a next-higher excited state with a femtosecond pulse has been observed.[12] According to the categorization,[15] one of these bands corresponds to the type-II STE, whereas the second one corresponds to the type III.

Although the combination of optical absorption, luminescence, and ESR measurements usually provides sufficient information to establish the model and some of the quantitative parameters of a point defect, experimental determination of the model for the luminescent state has not been successful so far. There are several factors that complicate the assignment of the model: first, the structure and character of the STE's are governed by the interaction and correlated behavior of their electron and hole components; second, the relaxation of an exciton or an electron-hole pair leads to formation of a pair of the primary defects: F center (the electron localized in the anion vacancy) and H center (the interstitial halogen atom).[3,4] As has been shown recently,[13] the triplet STE in NaCl exhibits RRS similar to those of F and H centers, suggesting that the STE may have the relaxed configuration only at the nearest F-H pair. Theoretical studies of the APES for the lowest state of excitons in different crystals may be of help in addressing some of these questions or, at least, to exclude a part of the alternative interpretations of the experimental data.

Many theoretical investigations of STE in alkali halides have been made since the pioneering work by Stoneham,[18] as reviewed by Williams and Song.[2] First, it has been assumed that the STE in alkali halides consists of a diffuse electron bound to a self-trapped hole or V_k center.[19] The V_k center can, itself, be considered as an X_2^- molecular ion (where X denotes a halogen atom) that occupies two anion lattice sites. This is the so-called (V_k+e) model. After the ENDOR experiments on the STE in KCl,[9] it has been shown that the (V_k+e) configuration, which has D_{2h} symmetry, is unstable. It is suggested that the STE is an off-centered (V_k+e),[9,20] in which the center of mass of the X_2^- molecular ion is displayed by ΔQ_2 along its molecular axis, as shown in Fig. 1. Extensive studies of the off-center model of the STE have been carried out by Song and Leung[21–23] on the basis of a one-electron pseudopotential extended-ion technique (EIT). These calculations have shown that the electron of the STE is localized in the crystalline potential rather than due to the interaction with the X_2^- molecular ion. Recent *ab initio* many-electron calculations[24–26] have supported this conclusion and simultaneously emphasized the importance of the many-electron approach to the problem. It has been shown that an X_2^- molecular ion, displaced from the D_{2h} position, is polarized in such a way that the hole is mainly localized on the anion located closer to the vacancy trapping the electron. As was discussed in Ref. 27, the trapping of an electron on a lattice anion site and the localization of the hole onto the anion displaced from this site may be considered as a common feature of the STE structure not only in the alkali halide crystals but also in silicon dioxide and lithium oxide.

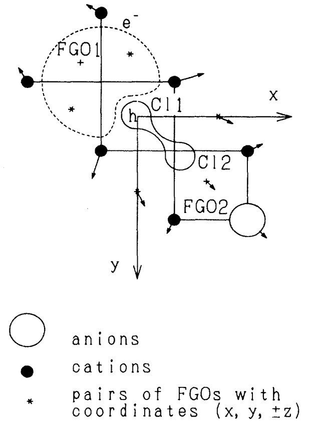

FIG. 1. Schematic presentation of the off-center model for the STE in alkali halide crystals. Open circles show anions, closed circles cations, crosses are floated orbitals on the (100) basis plane on which the X_2^- molecular ion, indicated by combined two circles, is located and asterisks show pairs of floating orbitals located on the (100) plane above and below the basis plane. Arrows show the directions of the displacements of ions from the lattice sites and of floating orbitals from their positions as the system is displaced from the D_{2h} configuration.

In this paper our intention is to extend these calculations in order to address some of the questions stated above. For this purpose we have chosen three chlorides: LiCl, NaCl, and KCl. According to the classification by the optical-absorption and luminescence properties of the STE,[14,15] they belong to different groups of alkali halides: in LiCl, type-II luminescence is emitted; in NaCl, type-I and type-II luminescence is emitted and the existence of the third minimum in the APES is suggested from recent femtosecond measurements,[12] and only type-III luminescence is emitted in KCl.

All of these crystals have been studied theoretically before; however, the results are still contradictory. In particular, recent calculations of the triplet STE in LiCl (Ref. 25) with the aid of the unrestricted Hartree-Fock method and ICECAP computer code have demonstrated the possibility of existence of an unexpected "compact" configuration of the STE. The peculiarity of this configuration is that, although it is off-centered, both the anion carrying the hole and the electron are located much closer to each other than has been predicted in the previous one-electron EIT calculations.[22] However, Baetzold and Song[28] have found that this configuration has higher energy than that corresponding to a much larger separation between the electron and the hole.

The EIT calculations[22] by Song and Leung showed that the STE's in NaCl and KCl have different configurations: the amount of the off-center displacement ΔQ_2 of the Cl_2^- molecular ion from the D_{2h} position is smaller in NaCl by as much as 1.5 Å than that in KCl and that the STE in KCl is more likely a nearest F-H pair. Recent calculations employing different many-electron *ab initio* techniques[26,28] have shown that the values of ΔQ_2 in both crystals are much smaller and closer to each other. On the other hand, recent RRS measurements suggest that the STE in NaCl (Ref. 13) is more likely an F-H pair. Therefore, despite the steady progress in the experimental and theoretical techniques, the models of the STE in these crystals remain unclear.

Since the studies by Pooley[29] and Itoh, Stoneham, and Harker,[30] the quantum-mechanical calculations of the decay of the STE into the F-H pair focused on the transfer of the X_2^- molecular ion along the direction of its molecular axis. Although it is a well-known experimental fact that the H centers may easily rotate,[31] this was not taken into account in the discussion on the process of the self-trapping and subsequent evolution of the *F-H* pair, in spite of the suggestion by Kabler and Williams.[32] Recently, it has been pointed out that the rotation of the Cl_2^- molecular ion may be one of the causes of the appearance of several minima on the APES of the STE.[12]

In view of the present situation where a comprehensive theoretical study of the multidimensional APES of the STE is still a difficult problem, we try to derive qualitative conclusions on the STE's in these crystals by comparing the existing experimental data with the results of calculation. It is intended to distinguish the points that can be definitely concluded and those which remain open.

II. METHODS OF CALCULATION

The existing *ab initio* calculations of the electronic structure of the STE in the alkali halide crystals[24-26] were mainly concerned with the validity of the off-center model of the STE. A relatively detailed calculation of the lowest APES for the triplet STE has been carried out for KCl (Ref. 26), only in the vicinity of the minimum of the adiabatic potential. In the present work, we are aiming to make a much more extended study, including not only investigation of the structure of the triplet STE but also of various configurations of the nearest *F-H* pairs and the barriers for the adiabatic transitions between these configurations. The ICECAP computer code that has been successfully used in our previous calculations is too time consuming for the present purpose. Therefore, we have developed an *ab initio* DICAP (defects in ionic crystals automated pseudopotential) computer code that makes the calculations for large quantum clusters several times faster than using the ICECAP code. The quantum-mechanical treatment of the exciton in both methods is absolutely equivalent. However, the DICAP code takes into account lattice distortion only in a finite region outside the quantum cluster where the displacements of ions from their sites are appreciable (more than 0.01 of the lattice constant). The positions of ions in the quantum cluster and in the surrounding distorted area are calculated using an automated energy minimization procedure that makes the calculation very efficient. The disadvantage of this approach is that the ions outside the cluster are treated as nonpoint frozen ions and do not polarize. Therefore, the DICAP code allows us to take into account only part of the polarization of the crystalline lattice by the exciton. It was extensively used for the search of the extreme points on the APES, and further calculations using the ICECAP code were made near the extreme for comparison. Let us give a brief account of the most important characteristics of both computer codes.

In both methods, the unrestricted Hartree-Fock-Roothaan equations (UHF) are solved for a molecular cluster (c) embedded in an infinite crystalline lattice (l). In ionic crystals, the lattice outside the quantum cluster is treated in the ionic approximation, i.e., the crystal electronic density is represented by the combination of densities of bare ions and the many-electron wave functions of these ions are strongly orthogonal to each other and to the wave function of the cluster. The lattice ions are located near the perfect lattice sites and treated using various approximations. In the approximation, which is used in both ICECAP and DICAP codes, the total energy of the crystal with a defect is calculated as

$$E=T_e+U_{ee}+\Sigma U_{e\text{-}c}+\Sigma U_{e\text{-}l}+\Sigma U_{c\text{-}l}+E_{\text{pol}} , \qquad (1)$$

where T_e is the kinetic energy of the electrons in the cluster, U_{ee} the interaction energy between the electrons in the cluster, $U_{e\text{-}c}$ the interaction energy between the electrons in the cluster with the cores (nuclei) of ions in the cluster, $U_{e\text{-}l}$ the interaction energy between the electrons in the cluster with the ions outside the cluster, $U_{c\text{-}l}$ the energies of the pair interactions between the cores of ions inside the cluster and the ions of the rest of the crystal, and E_{pol} the lattice polarization energy that occurs as a consequence of the incorporation of a defect within the cluster. In Eq. (1), c and l mean that the ion (core) belongs to the cluster or the rest of the crystalline lattice, respectively, and a summation is made over all the electrons and cores inside the cluster and all the ions outside. The energy of the pair interaction between the cores of ions in the cluster with ions outside it, $U_{c\text{-}l}$, may be presented as a sum of the Coulomb and short-range terms:

$$U_{c\text{-}l}=Q_cQ_l/R+U_{c\text{-}l}^{s\text{-}r} . \qquad (2)$$

The cores of ions within the cluster in both ICECAP and DICAP codes in the present calculations were described by the semilocal normconserving pseudopotentials of Bachelet, Hamann, and Schluter[33] (BHS) (although all electron calculations are possible with both codes). For the first three terms in (1), both methods calculate identically; the main difference between these two methods is in the treatment of the ions outside the cluster and hence in the remaining three terms.

In the ICECAP method, the crystalline lattice outside the cluster is treated in the Mott-Littleton approximation,[34] which is based upon a description of a lattice in terms of the classical shell model for ions and effective-pair or three-body potentials for the interaction between them. In these approximations each ion within the finite region outside the cluster (region II) is represented by the point core and shell, carrying the charges which are the parameters of the method. The sum of these charges is equal to the charge of the ion in the perfect lattice. Outside this region the lattice is treated as a polarizable dielectric continuum. The core and shell are connected by a spring having the elastic constant that corresponds to the polarizability of the ion in the lattice. Thus, the term $U_{e\text{-}l}$ in (1) corresponds to the interaction between the electrons localized within the cluster with the cores and the shells of ions in region II. By the dipole approximation, the polarization of the ions outside the cluster by the defect is represented by the displacement of their shells relative to the cores. The lattice distortion (the inertial part of the lattice polarization) is simulated by the core's displacement from their lattice-site positions. The term $U_{c\text{-}l}$ and the polarization energy, E_{pol}, are calculated employing the pair potentials for the interactions between the ions and the Mott-Littleton procedure by using the HADES code.[35] The parameters of these pair potentials were taken from Ref. 36. A thorough review of this technique has recently been published by Vail[37] and is discussed in Ref. 26.

The electronic structure of the cluster embedded in the polarized crystalline lattice and the lattice polarization by the electric field produced by the difference between the charge density distributions in the cluster simulating the defect and the perfect lattice are calculated sequentially as different steps of the computation procedure. Each new charge-density distribution in the cluster produces a new response by the polarizable lattice. To achieve consistency between these two factors, the dipole, quadrupole, and octopole moments of the new charge-density distribution within the cluster were calculated after each successful step of the UHF calculation of the electronic structure. They were compared with the moments produced by the charges of the shell-model ions located in the same positions as the cluster ions. The difference in the multipole moments was compensated for by generating additional charges situated in the core locations of the cluster ions. The altered ion charges were used to calculate the response of the lattice outside the cluster. In this way consistency of the multipole moments between the quantum-mechanical and the HADES-type representation of the charge-density distribution in the cluster area was achieved with a typical accuracy of about 10^{-5}. This required on average 5–7 iterations of the UHF-HADES self-consistency procedure.

In the DICAP method, the cations outside the cluster are represented by their BHS pseudopotentials, whereas the anions may either be treated by the whole-ion pseudopotential approximation or considered as point ions. In the present study, the point-ion approximation for the anions was used in all the calculations. This seems to be a reasonable approximation, since all the cluster electrons (including the excited electron of the exciton) are strongly localized within the cluster in most of the calculations and only slightly penetrate the anions of the second sphere of the surrounding lattice. At the same time the representation of the nearest cations by the semilocal pseudopotential is essential in order to prevent unphysical delocalization of the wave function of the excited electron outside the cluster. The summation of the matrix elements of the interactions of the electrons within the cluster with the pseudopotentials of cations and anions outside the cluster (the analogue of the Madelung sum) is performed over the infinite lattice using the conventional Ewald technique, whereas in ICECAP only a finite number of such ions is included.

A crystal with a defect in the DICAP method is simulated by a quantum cluster embedded in an infinite lattice of nonpoint ions interacting by pair potentials. Since the polarization of the ions outside the cluster is not taken into account, the parameters of their pair interactions should be slightly different from those for the lattice constructed from polarizable ions. The total set of parameters includes the parameters of the interaction between the cores of the ions inside the cluster with the ions outside the cluster and of the interaction between these ions. The analytical form of the pair potential in all cases considered was chosen as

$$U^{s\text{-}r}_{c\text{-}l} = A\exp(-aR) - C_6/R^6 \, .$$

The infinite crystal is effectively divided into three regions: (i) the quantum-mechanical cluster, which includes several ions strongly perturbed by the defect; (ii) the surrounding region, where the ions are considerably displaced from their sites but can be treated in the whole-ion pseudopotential approximation; (iii) the crystal remainder, which produces only a crystalline potential inside the first two regions mentioned above. The number of ions in the first two regions usually does not exceed several tens. Their displacements are optimized at each step of the calculation of the APES.

The parameters of the potentials were optimized in order to satisfy the following criteria: (i) the equilibrium geometry of the cluster simulating the perfect lattice has to coincide with the corresponding fragment of the infinite lattice; (ii) the total energy of this cluster has to behave symmetrically with respect to the displacement of the ions both inward and outward from the border of the cluster. In this way, the inequivalence between the interactions of the ion on the border of the cluster with the quantum-mechanical ions inside the cluster and with the ions represented by frozen pseudopotentials outside the cluster is corrected. The lattice constant obtained using these pair potentials and the HADES code for the KCl was calculated to be 3.07 Å, in good agreement with the experimental data (3.116 Å). The parameters of these pair potentials are summarized in Table I.

Such an approach to the calculation of the interactions between the "quantum-mechanical" ions and the rest of the ions has a substantial advantage provided that the ionic approximation holds with a high accuracy. Indeed, it makes the size of the cluster very flexible and allows us to change it without inducing jumps in the total energy of the system. In particular, in the process of the calculation of the APES, some of the frozen ions may easily be included in the geometry optimization, whereas some of them may be fixed in their lattice sites if their displacements appear to be negligibly small. Furthermore, more ions may be made quantum mechanical if their electronic structure is expected to change appreciably during the next step of the diffusion process. Simultaneously, some other ions may be frozen as whole-ion pseudopotentials if

TABLE I. Parameters of the short-range pair interactions (in atomic units) between ions and cores in KCl and NaCl crystals.

Crystal	a	b	A	α	C_6
KCl	K^+	Cl^{7+}	108.409	1.470	691.677
	Cl^-	Cl^{7+}	31.941	1.447	
	K^+	K^+	387.585	2.002	243.125
	K^+	Cl^-	213.302	1.632	598.365
	Cl^-	Cl^-	19.112	1.386	
NaCl	Na^+	Cl^{7+}	96.050	1.922	
	Cl^-	Cl^{7+}	49.966	1.478	
	Na^+	Cl^-	135.985	1.916	
	Cl^-	Cl^-	35.632	1.441	

they are not perturbed by the defect. Thus the cluster, i.e., the distorted region of the crystal lattice, follows the adiabatic path of the defect diffusion, changing the shape and altering the number of the quantum-mechanical and frozen ions. The flexibility of the model described above makes the study of the mechanisms of diffusion and transformation of the point defects in ionic crystals very efficient. The HADES and ICECAP methods have some difficulties here, since the explicit region I is always spherical; thus, a diffusion process requires a very large region; otherwise, the edge errors become large when the defect approaches the edge of region I.

As was noted in Ref. 26, the interaction between the cores of the ions represented by the pseudopotentials differs from the simple Coulomb form for heavy ions (see Ref. 38 for a review) and should be corrected by including the additional terms. In Ref. 26, to correct the interaction between the cores of K^+ and Cl^- ions, we have included the exponential repulsion term. However, as shown in *ab initio* calculations,[39] the polarization of the core of the potassium ion also plays an important role in the chemical bonding of the KCl molecule. Therefore, along with the repulsion term, the dispersion attraction also should be taken into account. The parameters for the core-core interactions between the ions considered in the present study are summarized in Table I. For the Li^+ and Na^+ ions, the dispersion term appeared to be negligibly small.

Ab initio calculations of the STE in various crystals have demonstrated the strong polarization of the X_2^- molecular ion during its transformation from the V_k configuration into the off-center configuration of the STE and subsequently into the H center. Following the adiabatic path, the anions pass through lattice-site and interstitial positions in which the values of the crystalline potential are substantially different. Therefore, the initial choice of the basis set of atomic orbitals (AO) for these ions plays a crucial role. According to our previous experience,[26] the split 511*sp* valence basis set on the chlorine ions provides a reasonable compromise between our computer facilities and the accuracy of the calculations. These basis sets have been obtained by independent variation of the exponents of the split set of 7*sp* Gaussians in the crystalline field for each particular crystal and then contracted into the 511*sp* form. Two split AO's are necessary to reproduce the polarization of the anions during the $(V_k+e)\rightarrow F\text{-}H$ transformation. Further optimization of the outer exponents at different points of the APES for the V_k center and the H center, as well as additional splitting of the basis set, does not lead to substantial changes of the system's total energy and the geometry of the defects.

Nevertheless, prior to the present calculations, we performed an additional study of the basis set and calculated the H center in LiCl using the ICECAP code for all-electron calculations and for calculations employing the BHS pseudopotentials and different basis sets. We were mainly concerned with the possible role of the d orbitals. Therefore, in the all-electron calculations, we employed the standard 6621*sp* basis set for the chlorine ions, which was extended by the d AO with the value of the exponent equal to 0.514. For the cations, we used both Huzinaga (4/4*s*) and 621*sp* basis sets. In the pseudopotential calculations, the optimized 511*sp* basis for chlorine and the Huzinaga (3*s*) basis for lithium were used. We did not find substantial differences between the geometries of the H center at various orientations and barriers for its rotation calculated using different basis sets and numbers of electrons. The population of the d orbitals was negligibly small. Although they certainly improved the polarizability of the anions, this did not substantially affect the results. Therefore, in all further calculations of the electronic structure of the H centers and the STE in LiCl, NaCl, and KCl using both the ICECAP and DICAP codes, we employed the 511*sp* basis sets for the chlorine ion and (3*s*) Huzinaga-type basis sets for cations. The latter were additionally optimized for the BHS pseudopotential by minimizing the energy of the isolated atoms. These basis

TABLE II. The parameters of the valence Gaussian basis sets for K^+, Na^+, Li^+ and Cl^- ions in KCl, NaCl, and LiCl crystals, optimized for use with the BHS pseudopotential.

K		Na		Li	
exponents	*s*-coeff.	exponents	*s*-coeff.	exponents	*s*-coeff.
0.1997	−0.342 210	0.437	−0.151 032	0.482	−0.120 248
0.074 18	0.504 407	0.0635	0.763 772	0.0759	0.617 720
0.0242	0.750 807	0.021	0.347 636	0.0278	0.479 348

	Cl^- in NaCl			Cl^- in LiCl	
exponents	*s*-coeff.	*p*-coeff.	exponents	*s*-coeff.	*p*-coeff.
3.8599	0.237 174	0.011 310	3.8599	0.281 105	0.013 367
2.3526	−0.746 874	−0.096 753	2.3999	−0.834 744	−0.100 795
1.1136	0.253 675	0.309 352	1.1136	0.275 003	0.321 392
0.481 09	0.692 630	0.640 832	0.490 76	0.505 986	0.599 440
0.28283	0.411 552	0.163 289	0.367 57	0.595 851	0.184 049
0.146 02	1.0	1.0	0.154 91	1.0	1.0
0.043 157	1.0	1.0	0.044 025	1.0	1.0

sets are compared in Table II. We should note that there is a sizable difference between the values of exponents and the ratio of coefficients, which reflects the difference in the compactness of the lattice and in the size of the cations.

The wave function of the excited electron of the STE changes very sharply according to the position of the X_2^- molecular ion. In particular, in the (V_k+e) configuration the electron occupies a very diffuse state, whereas in the off-center STE configuration its wave function is much more localized and becomes similar to the *F*-center wave function in the nearest- and the next-nearest-neighbor *F-H* pair configurations. As has been shown in the calculations for the STE in KCl,[26] the localization of the electron takes place gradually, following the off-center displacement of the hole component from the V_k center position. In order to follow the changes in the electron distribution, the basis set has to be flexible enough to allow different types of localizations. This may be achieved by employing a set of floating Gaussian orbitals (FGO's) centered in different sites within the cluster. For a methodical treatment, the best procedure would be to produce a universal basis set and to fix it in all the calculations of the APES of the system. However, in practice this seems to be impossible for several reasons. The main reason concerns the nature of the study, since we intend to consider a very large displacement of the X_2^- molecular ion from its (V_k+e) configuration to the *F-H* pair configuration. Therefore, the distances between the centers of the FGO's and the anions change very strongly. In particular, if one of the FGO's is permanently localized near the anion site[28] at some displacement of the V_k center, it comes very close to the FGO. In this region, the overlap integral between the FGO and the outer diffuse *s*-type AO of the anion becomes close to 1, and the overlap matrix of AO's becomes almost singular. This makes the UHF procedure unstable and may cause an artificial lowering of the energy in the vicinity of this point. Moreover, the combination of two closely centered *s*-type FGO's with similar exponents is in fact a *p*-type AO having the maximum, which may appear to be far outside the cluster where the cations are represented by the point ions. The population of this AO may also lead to the artificial lowering of the total energy of the system.

Therefore, in all present calculations we used more time-consuming but reliable procedures based upon the variation of the positions and exponents of the FGO's. As in the previous calculations,[25,26] in most cases we employed the basis of 10 *s*-type FGO's centered in interstitial positions within the cluster (see Fig. 1). The optimized exponents and positions of these FGO's are discussed for each particular case.

The total energy of a crystal with a STE in each APES point, using the ICECAP code, was obtained for given positions of nuclei of ions in the cluster and of the centers of FGO's, with the rest of the crystal relaxed according to the charge-density distribution in the cluster. After minimizing the total energy of the system relative to the FGO's positions and their exponents, the coordinates of ions in the cluster were changed in order to find the global minimum of the total energy or to calculate the energy in the configuration found previously using the DICAP code.

III. RESULTS AND CALCULATIONS

A. Properties of V_k and *H* centers

As has been mentioned in the Introduction, the number of experimental techniques that may provide some information regarding the structure of the STE is rather limited, although more abundant information on the structure of the *H* and V_k centers has been obtained. Recent experimental results of the resonance Raman scattering of the hole centers in several alkali halides and of the STE in NaCl (Ref. 13) have emphasized the importance of comparative study of the local vibrations that may be attributed to these species. Another important factor, which determines the process of decay of the STE into the *F-H* pair and may play a role in the structure of the STE, is the orientation of the *H* center. In KCl it is experimentally established that the *H* center is oriented along the ⟨110⟩ crystalline axis.[40] Recent ESR experiments[41] and optical-absorption data[42] have show that the *H* center in NaCl has the ⟨111⟩ orientation, whereas the data for LiCl still does not exist. There are only a few theoretical papers related to the study of *H* centers.[43] Therefore, as a part of this study we have undertaken an *ab initio* calculation of the structure and the vibrational frequencies of the V_k and *H* centers in LiCl, NaCl, and KCl and compared with the results of Raman spectroscopy[44] and resonant Raman spectroscopy.[42] A thorough description of the results of these calculations will be published elsewhere.[42] Here we will consider only the points related to the topic of the present paper.

As has been mentioned above, the *H* center in LiCl was studied by making an all-electron calculation, employing different basis sets, and using the BHS pseudopotential technique. Since the results of these calculations are very similar, we report only the data obtained using the pseudopotential technique and the basis set of AO's on chlorines and cations presented in Table II. The $Me_{10}Cl_2$ quantum cluster was used in both ICECAP and DICAP calculations of the V_k center and $Me_{14}Cl_4$ for those of the *H* center. Both clusters included the first sphere of cations surrounding each anion. In the DICAP calculations the second sphere of anions surrounding the *H* center was included in the calculation of lattice distortion. The calculations made using both ICECAP and DICAP codes gave very similar atomic structures. For the neutral *H* center the difference in the displacements of ions inside the quantum cluster obtained using both codes does not exceed 0.01 of the lattice constant. The ionic displacements outside the cluster differ in some cases by 0.02%. However, the latter comparison is not straightforward because of the difference in the description of the lattice distortion. The vibrational frequencies were calculated only for the stretching vibrations of the Cl_2^- molecular ion in each center, which may be measured by the RRS technique.

The structure of the *H* center in NaCl is depicted in

Fig. 2(a), which also contains the directions and magnitudes of displacements of the surrounding ions. Comparable values were obtained also for the *H* centers in other crystals, and we do not think that it is worth presenting them because they do not add new information. A thorough description of the lattice deformation around the V_k center in alkali halide crystals has been presented in previous publications.[45,25,26] Therefore, a result of this work with respect to this defect is the calculation of vibrational frequencies. The equilibrium distances between the chlorine ions in the Cl_2^- molecules of all the centers are given for the sake of comparison.

The calculations predict the ⟨111⟩ orientation for the *H* center in all three crystals. The reason for the discrepancy between the experimental and theoretical orientations for the *H* center in KCl may be twofold. As is clear from the structure of the center (see Fig. 2), nearest cations are strongly displaced from their sites by the presence of the additional interstitial atom. The cores of the potassium ions are certainly polarized. This effect was not taken into account in our pseudopotential calculations. In order to check this point, we have performed the calculations of the *H* center in KCl in the cluster that contained only two chlorine ions carrying the hole. The polarization of the ions was treated within the shell model. We have obtained the same ⟨111⟩ orientation of the center; however, the energy difference from the ⟨110⟩ orientation dropped to 0.1 eV. Another factor is the interaction of the chlorine ions comprising the hole with the two nearest anions on the ⟨110⟩ axis (*C*12 in Fig. 3). The importance of this interaction has been pointed out in the ESR studies of the *H* center in KCl.[39] They have indicated a substantial isotropic hyperfine interaction with the nuclei of these ions. However, in our calculations we do not get an appreciable spin-density redistribution from the Cl_2^- ion to the anions by the ⟨110⟩ axis. This may be due to the neglect of the electron correlation in our single-determinant UHF calculations. In fact, the interaction between the localized electron configuration obtained in our calculations and that corresponding to the hole transfer from *C*11 to *C*12 (see Fig. 3) may be strong.

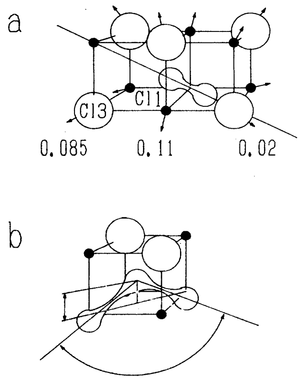

FIG. 2. (a) Model for the *H* center in Nacl. Arrows show the directions of the displacements of surrounding ions from the lattice sites. The numbers show that the magnitudes of the displacements are in the units of the lattice constant. (b) The saddle-point configuration for the *H*-center diffusion in NaCl.

The calculated vibrational frequencies are in satisfactory agreement with the available experimental data. The average accuracy of the vibrational frequency calculated using the Hartree-Fock method is usually expected to be 10%. The results of the calculation are in accordance with the experimental observation that the vibrational frequency of the *H* center is larger by about 30% than that of the V_k center. The experimental frequency for the *H* center in KCl is given for its ⟨110⟩ orientation. The apparent substantial difference between the frequencies of stretching vibrations of the Cl_2^- molecular ion in V_k and *H* centers results from two main factors. First, as is clear from Table III, the Cl_2^- molecular ion in the *H*-center configuration is much more compressed than in the V_k center. Second, the gradients of the crystalline potential acting on the molecular ion in both cases are different.[42]

In order to study the capability of our calculation methods to make correct predictions concerning the heights of the barriers for the STE decay and the *F*-*H* separation processes, we have calculated the adiabatic barrier for the *H*-center diffusion in NaCl using the DICAP code. The saddle-point configuration is schematically depicted in Fig. 2. It resembles a bent Cl_3^{2-} molecule. About 0.7 of the spin density of the hole is localized on the central chlorine ion, which is displaced from the *xy* plane by 0.39 Å. The angle between two Cl-Cl bonds in the quasimolecule is about 158°. Both Cl-Cl bonds are stretched; their length is equal to 2.66 Å. The height of the barrier is equal to 0.17 eV. Although this value is small, it is, nevertheless, much larger than the experimentally observed activation energy of 0.08 eV (Ref. 46) for the *H*-center diffusion in NaCl. Because of the hole localization on one anion at the saddle-point configuration, the barrier should become lower if we take into account the polarization of the lattice. However, this result indicates clearly that in the framework of the ionic model employed in the DICAP code, the barriers for diffusion motion of the Cl_2^- molecular ion in NaCl should be overestimated.

TABLE III. The characteristics of the V_k and *H* centers in LiCl, NaCl, and KCl. R_e is the equilibrium distance in the Cl_2^- molecular ion, ω the frequencies of the stretching vibrations of the Cl_2^- molecular ion in the centers, $\Delta E_{110-111}$ the energy differences between ⟨110⟩ and ⟨111⟩ orientations of the *H* center.

		R_e	ω^{th} (cm^{-1})	ω^{exp} (cm^{-1})	$\Delta E_{110-111}$ (eV)
LiCl	V_k	2.72	258		
	H	2.51	388.5		0.20
NaCl	V_k	2.74	256	258	
	H	2.52	390.3	361.4	0.27
KCl	V_k	2.73	241	241	
	H	2.60	314.3	328.8	0.17

B. Triplet self-trapped exciton

The results of recent *ab initio* calculations of the lowest triplet state of the (V_k+e) configuration (D_{2h} point) in several alkali halide crystals (LiCl, NaF, NaCl, NaBr, KCl) have indicated[26,28] that in the framework of the UHF method this configuration is unstable with respect to the displacement of the Cl_2^- molecular ion along the ⟨110⟩ crystalline axis. As has been discussed in Ref. 26, the single-determinant UHF method fails in the vicinity of the (V_k+e) configuration. In fact, the interaction of several electronic configurations has to be taken into account at this point in order to get a correct electronic energy. Therefore, the energy at the D_{2h} point does not provide a good starting value for the energy minimization. Nevertheless, we will assume that electron correlation is not vital far from this point and will make a critical analysis of the results obtained for the strongly off-centered configuration of the STE and the *F-H* pair. Some of these results will allow us to make additional comments regarding the D_{2h} point.

In view of the RRS results that the STE in NaCl is more likely an *F-H* pair and that several (at least three) types of luminescence are emitted from STE in alkali halides, we calculated the energy at various possible configurations of the STE, including the nearest-neighbor *F-H* pair. Since the most complete set of experimental data exists for the STE in NaCl and also the *H*-center configuration for NaCl is predicted properly, it was studied most carefully. The energy contour of the APES for the lowest triplet state of NaCl, in a wide range of configurations with respect to the translational motion and rotation of the X_2^- molecular ion, calculated using the DICAP code, is shown in Fig. 3. Atomic configurations corresponding to different points of the APES are schematically depicted in Fig. 4. The analysis of the APES indicates that both translational motion and rotation of the X_2^- molecular ion are important for determination of the positions of extreme points of the APES. For LiCl and KCl we have studied only the part of the APES near the minima usually attributed to the luminescent state (point *B* in Fig. 3). Let us first discuss this part of the APES.

We found that the minimum *B* of the APES appears for LiCl, NaCl, and KCl. Some of the numerical data, characterizing minimum *B* is these crystals, are summa-

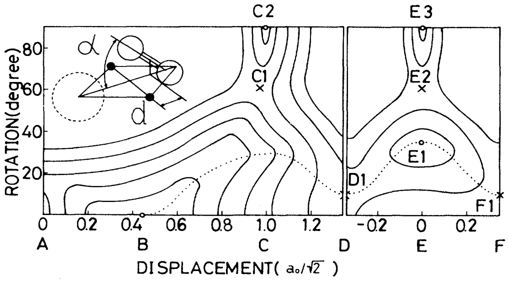

FIG. 3. A cut of the APES for the lowest triplet state in NaCl. The energy contours, by a separation of 0.1 eV, are presented in a coordinate system consisting of the *x* axis, the displacement *d* of the center of the mass of the Cl_2^- molecular ion along the ⟨110⟩ crystalline axis, and the *y* axis, the angle α between the Cl_2^- molecular axis and the ⟨110⟩ crystalline axis (see the inset). All other configuration coordinates, which determine the total energy of the system, including the molecular bond length, the torsion angle, the displacement of the center of mass relative to the axis, the displacements of the surrounding ions, and the positions and exponents of FGO's are optimized at each point of the APES. In the left-hand part of the figure the center of coordinate corresponds to the D_{2h} configuration (point *A*); in the right-hand part it corresponds to the nearest-neighbor *F-H* pair (point *E*). The point of APES minimum, the *F-H* pair, and the saddle points for the transfer to the next-nearest neighbor are denoted by *B*, *C*, and *D*, respectively; suffixes are added to denote the points with rotation. The atomic structures corresponding to these configurations are schematically depicted in Fig. 4. The dotted line corresponds to the minimum-energy trajectory for transformation from the STE to the *F-H* pair.

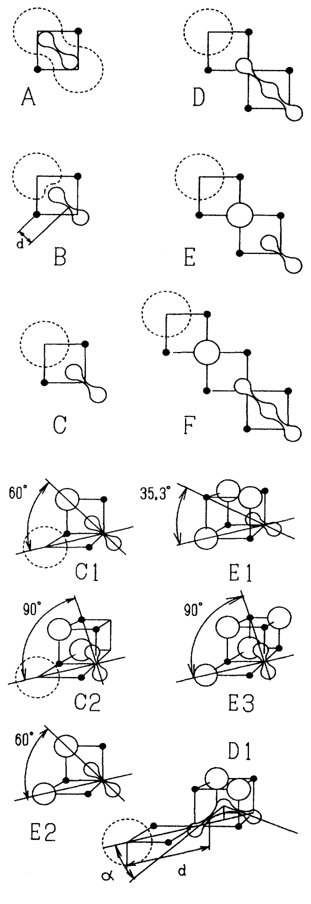

FIG. 4. The atomic configurations of the relaxed excitons relevant to the self-trapping process and formation of the *F-H* pairs for NaCl. *A*: the D_{2h} configuration; *B*: the minimum of the APES, the luminescence state; *C*, *C*1, *C*2: the nearest-neighbor *F-H* pair at different *H*-center orientations; *D*, *D*1: the saddle points for the transformation from the STE to the *F-H* pair; *E*, *E*1, *E*2, *E*3: next-nearest-neighbor *F-H* pairs with different orientations; and *F*, *F*1: the saddle points for further displacement of the *H* center.

TABLE IV. The positions (in units of the lattice constant), exponents, and Mulliken populations of two halogen ions and the Gaussian floating orbital *F*01 in the quantum cluster at the minimum of the APES.

	Coordinates			Exponents	Populations		
Crystal	*Cl*1	*Cl*2	*F*01	*F*01	*Cl*1	*Cl*2	*F*01
LiCl	−0.050; −0.050; 0.00	0.683; 0.683; 0.00	−0.70; −0.70; 0.00	0.09	7.114	7.822	0.733
NaCl	−0.113; −0.113; 0.00	0.557; 0.557; 0.00	−0.75; −0.75; 0.00	0.089	7.048	7.802	0.696
KCl	−0.029; −0.029; 0.00	0.599; 0.599; 0.00	−0.76; −0.76; 0.00	0.093	7.258	7.861	0.530

rized in Table IV. For NaCl and KCl, the configuration is stable with respect to rotation of the Cl_2^- molecular ion in the horizontal and vertical planes. In LiCl the shape of the APES is more complicated. It is indeed very soft in the wide range of coordinates including the rotation of Cl_2^-. A similar trend has been observed in recent calculations of the STE in LiCl by Baetzold and Song.[28] Provisionally, we have located the minimum at the ⟨110⟩ orientation of the Cl_2^- molecular ion. However, according to our preliminary results, the Cl_2^- molecular ion may be tilted by some angle towards a ⟨111⟩ direction. Additional studies are needed to make more precise assignment. The lack of experimental data makes this point not very important for the present discussion. Both experimental and theoretical studies of the STE in LiCl are currently in progress.

The position of minimum *B* and the parameters shown in Table IV were obtained first by the DICAP method and were used afterwards as initial parameters for the APES coordinate optimization within the ICECAP code. Both methods gave the same results. Present results for KCl practically coincide with those obtained in previous calculations.[26] The qualitative character and the degree of polarization of the Cl_2^- molecular ion in these three crystals are similar. They have to be treated with care, since the Mulliken population analysis was used in the calculations of the populations of the ions, which carry diffuse AO's. The electron component of the exciton is localized mainly on five floating orbitals as depicted in Fig. 5(a), although about 15% of the spin density is contributed by the *s*-type orbitals of the cations, surrounding the anion vacancy. Thus, minimum *B* represents a triplet excited state in which the hole is localized preferentially on one of the anions of the Cl_2^- molecular ion, occupying the intermediate position between the V_k and *H*-center configurations. The excited electron, on the other hand, is attracted to the vacant anion site adjacent to the hole.

The distance between chlorine ions *Cl*1 and *Cl*2 (see Fig. 1) in the Cl_2^- molecular ion is slightly different from that in the V_k center, but still much larger than that in the *H* center. Strong polarization makes the chemical bond of Cl_2^- weaker, which results in smaller frequencies of the stretching vibrations as compared with the V_k center. We should note that the distances δ between the vacant site and the anion *Cl*1 in LiCl and NaCl are similar and substantially smaller than in KCl (see Table V). The calculated energies of the Franck-Condon transition of the electron from the lowest state to the next-higher state and of the triplet luminescence (Franck-Condon transition of the electron to the singlet ground state) are presented in the last two columns of Table V. Both optical absorption and luminescence energies correspond to the π polarized transitions. They are close to but systematically larger than the experimental values for the triplet STE in the corresponding crystals, type II for LiCl and NaCl and type III for KCl.

The adiabatic displacement of the Cl_2^- molecular ion

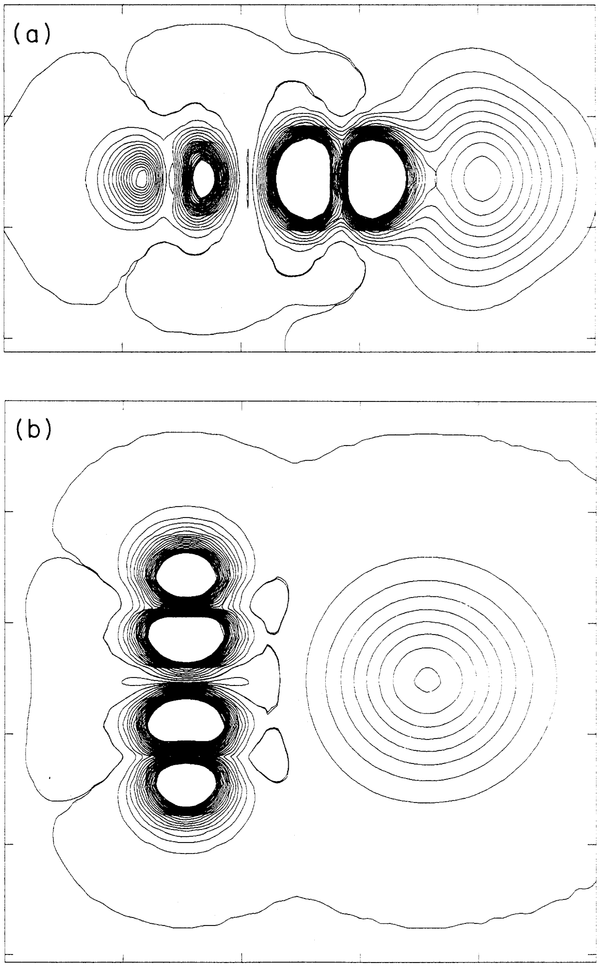

FIG. 5. The spin-density maps for STE in NaCl (a) at the minimum of the APES, a cut in the (100) plane, (b) at the nearest-neighbor *F*-*H* pair configuration with the *H* center reoriented by 90° a cut in the (211) plane.

TABLE V. The characteristics of the STE in LiCl, NaCl, and KCl. $R_{C11-C12}$ is the equilibrium distance between $C11$ and $C11$; ΔQ_2 is the distance between the center of mass of the molecule and the anion site in which the electron component is localized, whereas δ is the distance between $C11$ and the anion site; ω is the frequency of stretching vibrations of the STE; ΔE_{opt} and ΔE_{lum} are the energies of π polarized optical absorption due to the electron transition and of the triplet luminescence of the STE.

	$R_{C11-C12}$ (Å)	ΔQ_2 (Å)	δ (Å)	ω_{str} (cm^{-1})	ΔE_{opt} (eV) theor.	ΔE_{opt} (eV) expt.	ΔE_{lum} (eV) theor.	ΔE_{lum} (eV) expt.
LiCl	2.65	1.15	1.63		2.8	2.2	4.4	4.18
NaCl	2.64	0.87	1.53	218	2.6	1.95	3.8	3.51
KCl	2.77	1.26	2.08	206	2.0	1.87	3.2	2.31

toward the vacant anion site, where the electron is localized, increases the total energy of the system, as indicated by curve 1. The hole becomes even more localized on $C11$, which is accompanied by substantial weakening of the chemical bond with $C12$. The lattice distortion following this asymmetric charge-density distribution bears an increasing resemblance to a one-center exciton localized on anion $C11$. The bond between $C11$ and $C12$ becomes longer and essentially no bond is formed when the center of the mass of $C11$-$C12$ passes the origin of the coordinates in Fig. 1. The shape of the cut of the APES corresponding to the displacement of $C11$ and the adiabatic relaxation of all other surrounding ions is shown in Fig. 6, of which the horizontal axis is the same as that of Fig. 3. Curve 2 in the figure is the APES for the configuration in which the hole is localized on $C12$ and the electron near the anion vacancy adjacent to the hole. The configurations on curves 1 and 2 having the same energy represent two physically equivalent configurations of the electron and the hole. The single-determinant wave functions for curves 1 and 2 having the same configurations are not orthogonal. In the artificial crossing region, the substantial interaction between these configurations (or, in other words, the electron correlation) should lead to a spitting of the two curves (in fact, surfaces), which is qualitatively depicted in Fig. 6 by two broken curves.

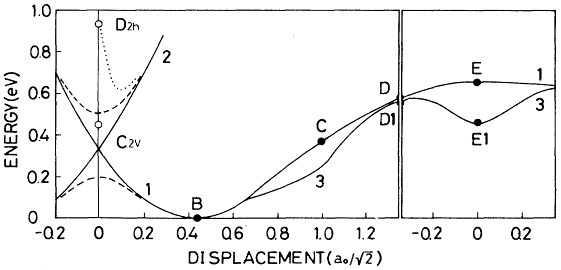

FIG. 6. Cuts of the APES for the lowest state of the exciton in NaCl (see Fig. 4). Curve 1 is that for the displacement of the Cl_2^- molecular ion along the ⟨110⟩ molecular axis (x axis in Fig. 4); curve 2 is that for the UHF solution with the opposite polarization of the electron and the hole components (see discussion in text); curve 3 is the energy vs configuration relation when the configuration is changed along the dotted line in Fig. 4; and the dotted line is that for the compact model of the STE in the vicinity of the D_{2h} configuration.

Two other energies, denoted D_{2h} and C_{2v}, are shown on the same energy axis for the sake of comparison. The first corresponds to the UHF energy of the (V_k+e) configuration obtained with the restriction that both the nuclei and the electronic wave functions have D_{2h} symmetry. The second is a so-called broken-symmetry solution of the UHF equations corresponding to D_{2h} symmetry of the nuclei and C_{2v} symmetry of the electronic wave function. The latter, in fact, is very similar to the adiabatic configuration, having lower energy. The significant energy difference between the D_{2h} and C_{2v} configurations emphasizes the importance of the electron correlation near the saddle point for the diffusion of the STE between the two nearest anion lattice sites (see the Appendix). The correct electronic configuration at this point should have a D_{2h} symmetry and an energy lower than the D_{2h} point calculated in this paper. It may be obtained using the configuration interaction technique developed for nonorthogonal determinantal wave functions in Ref. 47. We should stress that the electron correlation is important not only in the D_{2h} configuration but has to be taken into account in all points of the APES. Calculation only at the D_{2h} point may significantly distort the shape of the soft APES.

This comment allows us to clarify the nature of the compact model of the STE suggested in Ref. 25. Indeed, it corresponds to the minimum on the dotted curve in Fig. 6 and has been also obtained in our present calculations for LiCl. As is clear from the previous discussion, its existence entirely depends on the energy of the D_{2h} point. In all calculations published so far, it was treated as a starting point for the APES calculation. In this case, some of the points of the APES between the D_{2h} point and curve 2 have an energy lower than the UHF energy at the D_{2h} point. This was observed in Ref. 25. However, a proper account of the electron correlation may change even the qualitative behavior of the APES in the region of the configuration coordinates close to D_{2h} symmetry. Therefore, the shape of the APES as well as the validity of the adiabatic approximation in this region requires further study.

As has been pointed out in Ref. 48, in the framework of the off-center model of the STE, the mechanism for its diffusion in alkali halides may be considered as consisting of two steps: (i) a joint motion of the electron and the hole along the ⟨110⟩ axis (the barrier for this was just discussed in the preceding paragraph); (ii) rotation of the Cl_2^- molecular ion of the STE, which changes its direction by 60° (see Fig. 7); the latter resembles the 60° reorientation of the V_k center. Although the observation of diffusion of the STE is rather problematic,[49,50] we have simulated its 60° reorientation in NaCl for the sake of comparison with the V_k center and the H center. The calculations were made using the DICAP code. The atomic configuration at the adiabatic saddle point is shown in Fig. 7(b). It is perturbed, in comparison with that for the H center (see Fig. 2), by the presence of the electron component of the STE. If described in the same terms as the H center, it is also essentially the Cl_3^{2-} configuration where the hole is mainly localized on the central chlorine ion. The angle between the bonds of the central chlorine to the other chlorines is 140°, whereas the lengths of these bonds are 2.7 Å. The height of the central chlorine atom with respect to the plane [see Fig. 7(b)] is 0.81 Å. All these structural parameters as compared to those obtained for the H center reflect a strong attraction between the electron and the hole components of the STE. However, the height of the barrier obtained is 0.44 eV, which is much larger than the experimentally observed activation energy for the STE diffusion in NaCl of 0.15 eV,[50] and much closer to the characteristic values for the V_k center [0.40 eV for NaCl (Ref. 50)]. These results show clearly that the exciton relaxation energy and even the shape of its APES cannot yet be calculated with sufficient accuracy in all cases. If the off-center model of the STE is valid, the barriers for both the exciton transfer between two equivalent positions along the (110) axis and its 60° reorientation should be less than or equal to 0.15 eV. Therefore, the proper calculations of the electron correlation should lower the position of the D_{2h} point in Fig. 6 by about 0.8 eV. Electron correlation may considerably change the overall shape of the APES.

Finally, we should make some notes with respect to the dependence of the basis of FGO's on the configuration of the minimum B. Their value of exponents and positions were optimized at each point of the APES. In fact, the energy of the system depends most significantly on the parameters of $F01$. Its position and value of the exponent are more effective in determining the energy of the electron component of the STE and the total energy, respectively. Other FGO's also change their positions, following the displacements of the ions. The directions of their displacements from their respective positions at the D_{2h} symmetry are shown in Fig. 1. The values of the exponents remain approximately the same and close to 0.150 in LiCl, 0.128 in NaCl, and 0.125 in KCl. At the minima of the APES the populations of five FGO's surrounding $C12$ are close to zero and their presence does not affect the results of calculations. Therefore, we did not include them in further calculations of the F-H pair.

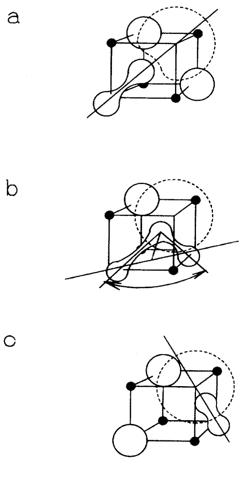

FIG. 7. A schematic presentation of the process of 60° reorientation of the STE in NaCl. (a) The initial configuration; (b) the saddle point; (c) the final configuration.

C. *F-H* pair and defect separation

The study of the APES for several configurations, shown in Fig. 6, with further separation of the electron and the hole components of the STE to form the nearest-neighbor and the more distant F-H pair was performed for NaCl and KCl. In the KCl case, we considered only the adiabatic diffusion of the Cl_2^- molecular ion along the $\langle 110 \rangle$ crystal axis, namely, only for configurations on the x axis of Fig. 6. The principal results of this study, which was made using the ICECAP code, may be summarized as follows.

(i) The next minimum on the APES along the $\langle 110 \rangle$ axis is located at the position corresponding to the next-nearest-neighbor F-H pair (configuration E).

(ii) The energy at the saddle-point configuration (configuration D) obtained is higher than that at B by 0.54 eV. This is the height of the barrier that the Cl_2^- molecular ion needs to overcome in order to reach from configuration B to the next-nearest-neighbor F-H pair by the axial displacement, and considered to be too high in view of experimental observation[51] as discussed later.

(iii) If we allow the H center to diffuse like in NaCl, i.e., through the out-of-plane saddle point (see Fig. 2), the height of the barrier is about three times smaller and equal to 0.18 eV. However, this result may also reflect the fact that we do not reproduce the correct orientation of the H center in KCl.

(iv) At configuration E, the ground singlet state of the crystal, calculated taking into account the lattice polarization, is located only about 0.1 eV lower than the triplet state. This excludes the possibility that this state is the luminescent state of the STE.

A more comprehensive study has been made for NaCl, employing the DICAP code. The numerical data obtained in this study are summarized in Figs. 4, 5, and 6 and Table VI. These results clearly indicate the importance of the reorientation of the H center. The most compact stable configuration of the nearest F-H pairs is schematically depicted in Fig. 4 ($C2$). It corresponds to the H center located in the site nearest to the F-center anion and reoriented by 90° with respect to the initial Cl_2^- molecular axis (henceforth, we will refer to it as the 90°

TABLE VI. The energies of different points of the APES for NaCl (see Figs. 3 and 4) relative to the STE minimum (eV). Point $E3$ is equivalent to $E1$; point $E2$ is equivalent to E.

A	B	C	$C1$	$C2$	D, $D1$	$E1$ ($E3$)	E ($E2$)	$F1$	G
0.34	0.0	0.38	0.54	0.29	~0.6	0.46	0.66	0.63	0.44

configuration). The H center in this configuration is oriented along the $\langle 111 \rangle$ axis.

In the course of the calculation of the APES, we have also examined two other nearest-neighbor F-H pair configurations: the nearest-neighbor F-H pair in which the Cl_2^- molecular ion is displaced axially [see Fig. 4 (C)] and that in which the H center is rotated by 60° into another $\langle 110 \rangle$ axis [Fig. 4 ($C1$)]. The latter configuration was suggested in Ref. 13 as a possible candidate for the STE configuration responsible for the experimentally observed RRS spectra. According to our calculations, both configurations are unstable and without any barrier for conversion into configuration B. The energy difference between configuration B and $C1$ is 0.54 eV. We obtained the height of the energy barrier for transformation from B to configuration $C2$ to be the same. The barrier for the transformation from $C2$ back to B is 0.25 eV. These barriers are too high in comparison with the activation energies for conversion from the luminescent states of the STE to the F-H pair as estimated on the basis of the temperature dependence of the radiation-induced luminescence and defect formation [typical values are <0.1 eV (Ref. 51)]. This may be due to the fact that the lattice polarization was only partly taken into account in the DICAP calculations. In order to check this point we have made calculations for configuration C using the ICECAP code. The energy difference between configurations B and C obtained was 0.32 eV, only smaller by 0.06 eV than the 0.38 eV obtained by a DICAP calculation. This difference gives an idea of how the results of the DICAP calculations may be affected if the lattice polarization for the neutral F-H pair is taken into account completely. Large (about 0.5 eV) values of the adiabatic barriers for the STE decomposition into the nearest-neighbor F-H pair calculated in both NaCl and KCl are presumably due to two factors which were not taken into account: electron correlation in the barrier region and polarization of the ion cores. The significance of the second factor comes from the comparison of the results of the ICECAP and DICAP calculations, using pseudopotentials, with the all-electron calculations.[28] The latter demonstrated qualitatively much softer behavior of the APES for the STE. However, lack of the calculated points of the APES in Ref. 28 prevents us from making more quantitative comparisons.

The energy of the Frank-Condon transition from the triplet to the ground singlet state for the 0° F-H pair (configuration C), which is not stable, is about 1 eV, whereas for the 90° F-H pair it is very close to zero. Therefore, these states cannot serve as initial states for the π luminescence in NaCl, in which the maximum of the luminescence band occurs at 3.51 eV. The potential well for the electron of the 90° F-H pair resembles that for the F center more closely than that of the STE [see Fig. 5(b)]. The lowest energy for its optical excitation is calculated to be about 3.0 eV, which is much closer to 3.15 eV obtained in our calculations for the single F center (the experimental value is 2.88 eV).

IV. DISCUSSION

Before we start a comparative discussion of the theoretical results obtained in this study with the experimental data, let us make some final remarks with respect to the accuracy of the theoretical method. Basic approximations employed in the present calculations are the single-determinant UHF method and the pseudopotential technique. Using these approximations, we have made an extensive study of the APES for the STE and the nearest defect pairs possible. However, as is clear from the results, the electron correlation and the polarization of the cores of cations (especially for KCl) may play an important role. In order to improve the quality of calculations, one needs to include all the core electrons and s,p,d valence basis set for cations and the configuration interaction at least at several points of the APES. This would make the calculations, in the framework of the methods employed in this study, almost impracticable. However, we believe that some qualitative conclusions may be made on the basis of the results obtained in this study: (i) The reorientation of the X_2^- molecular ion of the STE is an important factor that has to be taken into account in the construction of the atomistic model of the STE in alkali halides; (ii) in the STE configuration that emits the STE luminescence, the displacement of the X_2^- molecular ion should be less than that for the nearest-neighbor F-H pair configuration; (iii) the off-center model of the STE is valid but the real position of the X_2^- molecular ion and the degree of its polarization cannot be reliably evaluated by the present technique. However, a reasonable agreement of the calculated optical excitation and luminescence energies with the experimental data suggests that the models for the STE in LiCl, NaCl, and KCl may not change drastically after the method is improved. The consistency of the results for three crystals [or five, if we take into account the calculations for NaF and NaBr (Ref. 28)] also suggests that the present models may provide a good basis for further discussion of the experimental results.

As described in Sec. I, relaxed configuration of the STE in alkali halides have been classified into three groups, types I, II, and III, on the basis of the Stokes shift[14] and of the Ivey-Mollwo plots of the transition energy of the electron.[15] Evidently, type I and type II or III have different characteristics. Type I has a high luminescence energy and relatively small optical-absorption energy[52] for the electron, and coexist with other relaxed configurations in many alkali halides, indicating that type I and others originate from different structures. The difference between characteristics of types II and III is not as significant as that between type I and the others. However, the coexistence of types II and III observed in RbI (Refs. 16 and 17) and NaCl (Ref. 12) suggests that the classification is meaningful. Studies of both thermal and dynamic transfer between the type-II and type-III STE's in these materials indicate that both are on the lowest APES of the STE's. Although singlet luminescence dominates from type I, and triplet luminescence dominates from types II and III, recent experiments[53,54] show that both singlet and triplet luminescence is emitted from each relaxed configuration. Thus, we are tempted to consider that the APES's for the singlet and triplet states have minima of the same nature; only the depths are different, as confirmed by Baetzold and Song.[24] Earlier, the type-I relaxed state or the σ luminescent state of the STE has been suggested to be (V_k+e) at the D_{2h} configuration with electrons excited to $2s$,[18] and recently to be that with electrons excited to $1s$.[55] The latter suggestion is contradictory to the results of theoretical calculations, which indicate that the APES takes a maximum at the D_{2h} configuration. Although a minimum appears in the upper branch of the APES (see Fig. 6), the transition to the ground state is forbidden. For assignment of the origin of the type-I relaxed configuration, further calculation of the electronic states at the D_{2h} configuration taking the configuration interaction into account is necessary.

According to the classification of the relaxed configuration, the triplet luminescence in KCl is emitted from the type-III relaxed configuration and that in LiCl and NaCl from the type-II configuration. The only difference in the nature of the minima of APES for LiCl and NaCl and those for KCl is in the distance of the off-center deviation. This result suggests that the main distinction between types II and III results simply from the difference in the values of the off-center displacements. Alternatively, in view of the experimental results of the oscillation between the two relaxed states for NaCl, one may presume that two minima appear in the APES for the lowest state of the exciton in NaCl. The anomaly on the APES for NaCl, at a configuration where the molecular axis is slightly reoriented, suggests that there may be another minimum. If this is the case, the oscillation is between the off-centered configuration with a small (about half of the halogen-halogen distance) displacement without reorientation and another off-center configuration with a larger deviation and a slight reorientation. Furthermore, a minimum in the lowest APES at a reoriented configuration could appear for KCl, in which only the luminescence from the type-III relaxed configuration is observed. A search for such a minimum was not carried out because of the difficulty of assigning the correct orientation of the *H* center in KCl.

So far, it has not been possible to assign the atomic structures of the type-II and type-III relaxed states of the STE theoretically. As has been shown in the present calculation, as well as in previous calculations, the APES near the minima is extremely flat against the translational motion of the X_2^- molecular ion. Thus, accurate calculations to locate the minimum are extremely difficult at the present stage. On the other hand, the flatness of the APES leaves the possibility of inducing multiminima APES.

Present investigation appears to indicate that neither the type-II nor the type-III relaxed configuration of the STE is the nearest *F-H* pair, in spite of several suggestions;[21] the nearest *F-H* pair configuration having the axial symmetry [Fig. 4 (*C*)] does not exhibit a minimum and, furthermore, the luminescence energy emitted at this configuration, if any, should lie in the infrared range. After reorientation of the X_2^- molecular ion at the nearest-neighbor configuration by 90° [Fig. 4 (*C*)], the nearest neighbor *F-H* pair in NaCl becomes stable. However, again the calculated luminescence energy is too small and, hence, this configuration cannot be the candidate for either the type-II or type-III relaxed configuration.

The Raman spectra of STE in NaCl in resonance to the hole transition is known to exhibit a spectrum similar to the *H* center of NaCl. The result appears to conflict with the present investigation, which indicates that the stretching vibration frequency of the Cl_2^- molecular ion is more likely that of the V_k centers (see Tables III and IV). Although in the RRS experiments the decay-time constant of the Raman spectrum is shown to be the same as the decay time constant of the luminescence, the possibility that the type-II relaxed configuration and another APES minimum, corresponding to an *F-H* pair, are in thermal equilibrium at 80 K, where measurement was made, cannot be excluded. In fact, the optical-absorption spectrum for the self-trapped excitons of NaCl exhibits two prominent bands in the wavelength region of the hole transition,[55] but the RRS was measured for only one of the peaks. Further studies of the optical-absorption spectra and the Raman spectra in resonance to each optical-absorption band will reveal further details of the structure of the STE's in NaCl. Measurements of RRS for other alkali halides are of interest.

The present investigation has revealed general features of two-dimensional APES for the STE of NaCl with respect to the displacement and rotation of the X_2^- molecular ion. Evidently, as the X_2^- molecular ion is displaced to the nearest-neighbor *F-H* pair position, it becomes unstable against rotational motion; the only stable nearest-neighbor *F-H* pair is the X_2^- molecular ion oriented along the $\langle 111 \rangle$ direction perpendicular to the molecular axis. In view of the potential contours shown in Fig. 3, it is likely that the displaced X_2^- molecular ion is rotated 90° before reaching the nearest-neighbor configuration. This rotation can explain the low yield of stable (distant) *F-H* pairs in NaCl. We note also that the rotational motion of the X_2^- molecular ion, by relatively small angles, plays an important role in its translational motion as a replacement sequence, as first suggested by Kabler and Williams.[32] Further studies on this point for alkali halides in which the yield of the *F-H* pairs is high is of interest.

Although establishment of the models of the STE's in alkali halides is not yet attained, the present investigation has revealed some important features of the STE's. First of all, not only the change of the wave functions for the electron but also that of the hole is taken into account in order to discuss the electronic structures of the type-I STE, in particular. Both type-II and type-III STE's are off-centered (V_k+e); type-III has a possibly small reorientation. Rotation of the X_2^- molecular ion at the nearest-neighbor *F-H* pair configuration should be considered in order to explain the dynamics of the *F-H* pair formation from the STE.

Further experimental and theoretical efforts for elucidating the atomic and electronic structures of the STE's are needed. It is of particular importance to determine the relative locations of the electron and hole components. Accurate determination of the axis of the X_2^- molecular ion with respect to the position of the vacancy and of the symmetry of the wave functions of the electron at the 2*p* excited states with respect to the molecular axis will be of use in determining the structures. The dynamic studies of transfer between two relaxed configurations, as observed by Tokizaki *et al.*, will give further insight into this problem, if the change in the orientation of the X_2^- molecular ion during the transfer is clarified. The accuracy of the many-electron calculation at the present stage is not sufficiently high to elucidate electronic and atomic structures of the relaxed configurations of the STE's. It would be more important to make clear the elementary processes that play a role in the dynamical properties of the STE's. For instance, the pseudo-Jahn-Teller instability of the on-center STE is not adequately understood, in the circumstance where the polarization of the hole plays a role. Even though the theory cannot explain the presence of a variety of relaxed configurations, we consider that the flatness of the APES near the STE minimum leaves the possibility that multiminima appear if methods of calculation are improved. Because of the flatness, the STE will continue to be an interesting system in which the details of the dynamics of the defect reaction can be revealed.

ACKNOWLEDGMENTS

This work was supported partially by a program of the Ministry of Education, Science and Culture of Japan. A.L.S. acknowledges the Canon Foundation in Europe, the Royal Society, and the Royal Institution of Great Britain for financial support. The authors are grateful to A. H. Harker, R. C. Baetzold, and E. N. Heifets for valuable discussions and to R. C. Baetzold and K. S. Song for sending a copy of their manuscript prior to publication.

APPENDIX: CONFIGURATION INTERACTION NEAR THE D_{2h} CONFIGURATION

The nature of the wave functions for the lower and upper branches of the APES for the broken symmetry at the D_{2h} configuration is discussed in this section. The broken-symmetry solutions at the D_{2h} configuration may be written as determinants in terms of electron and hole wave functions *e* and *h* as

$$\begin{aligned} \Phi_L &= |h_L e_L| , \\ \Phi_R &= |h_R e_R| , \end{aligned} \tag{A1}$$

where suffixes *L* and *R* indicate the wave functions of the two electronic configurations corresponding to the localization of the electron and hole to the left (*L*) and right (*R*) of the vertical mirror plane passing through the center of the coordinates (see Fig. 1). The two states are degenerate at the D_{2h} configuration and the degeneracy is removed by configuration interaction. Using nonorthogonal configuration interaction, the resulting wave functions are

$$\begin{aligned} \Psi_1 &= \Phi_L + \Phi_R , \\ \Psi_2 &= \Phi_L - \Phi_R , \end{aligned} \tag{A2}$$

and the energy splitting $\Delta E = E_1 - E_2$ is

$$\Delta E = 2\frac{ES - \langle \Phi_L | H | \Phi_R \rangle}{1 - S^2} , \tag{A3}$$

where $S = \langle \Phi_L | \Phi_R \rangle$ is the overlap integral and *H* the Hamiltonian.

At the lowest state of STE, the electron wave function is even parity and the hole wave function is odd parity. The electron and hole wave functions under broken symmetry are unsymmetrized by admixture of wave functions of opposite parity and hence are given by

$$\begin{aligned} h_L &= h_u + \alpha h_g , \\ h_R &= h_u - \alpha h_g , \\ e_L &= e_g + \beta e_u , \\ e_R &= e_g - \beta e_u . \end{aligned} \tag{A4}$$

Thus the wave functions Φ_L and Φ_R are given by linear combinations of the lowest state of STE $|h_u e_g|$, the electron excited state $|h_u e_u|$, the hole excited state $|h_g e_g|$, and the double excited state $|h_g e_u|$,

$$\begin{aligned} \Phi_L &= |h_u e_g| + \beta |h_u e_u| + \alpha |h_g e_g| + \alpha\beta |h_g e_u| , \\ \Phi_R &= |h_u e_g| - \beta |h_u e_u| - \alpha |h_g e_g| + \alpha\beta |h_g e_u| . \end{aligned} \tag{A5}$$

Putting Eq. (A5) into (A3), we obtained an energy separation ΔE of

$$\begin{aligned} \Delta E = \frac{2}{M(1-S^2)} \{ & \alpha^2 (1+S) \Delta E_e + \beta^2 (1+S) \Delta E_h \\ & - \alpha^2 \beta^2 (1-S) \Delta E_2 \\ & + \alpha\beta (1-S)(J_0 - K_0) \\ & - \alpha\beta (1+S)(J_1 - K_1) \} , \end{aligned} \tag{A6}$$

where ΔE_e is the excitation energy of the electron to the odd parity excited state, ΔE_h that of the hole to the even parity excited state, and ΔE_2 is that of double excitation. The last two terms are the correlation interaction; J_0 and K_0 are the Coulomb and exchange interaction energies between the ground and double excited states and J_1 and K_1 are similar energies between the electron and hole excited states. *M* and *S* are the overlap integrals and are given by

$$M=(1+\alpha^2)(1+\beta^2)\ ,$$

$$S=M^{-1}(1-\alpha^2)(1-\beta^2)\ ,$$

respectively. Clearly, the separation between the upper and lower branches arising from the configuration interaction is somewhat smaller than the electron and hole transition energies. We found also that for the relaxed broken-symmetry solution, the halogen-halogen separation is larger than that for the symmetry solution, which gives approximately the X_2^- molecular ion.

---

[1] N. Itoh, Adv. Phys. **31**, 491 (1982).

[2] R. T. Williams and K. S. Song, J. Phys. Chem. Solids **51**, 679 (1990).

[3] N. Itoh and K. Tanimura, J. Phys. Chem. Solids **51**, 717 (1990).

[4] Ch. B. Lushchik and A. Ch. Lushchik, *Decay of Electronic Excitations with Defect Formation in Solids* (Nauka, Moscow, 1989).

[5] N. Itoh, A. M. Stoneham, and A. H. Harker, Surf. Sci. **217**, 573 (1989).

[6] M. J. Marrone, F. W. Patten, and M. N. Kabler, Phys. Rev. Lett. **31**, 467 (1973).

[7] D. Block and A. Wasiela, Solid State Commun. **28**, 455 (1979).

[8] R. W. Williams and M. N. Kabler, Phys. Rev. B **9**, 1897 (1971).

[9] D. Block, A. Wasiela, and Y. Merle d'Aubigne, J. Phys. C **11**, 4201 (1978).

[10] R. T. Williams, J. N. Bradford, and W. L. Faust, Phys. Rev. B **18**, 7038 (1978).

[11] R. T. Williams, Opt. Eng. **28**, 1024 (1989).

[12] T. Tokizaki, T. Makimura, H. Akiyama, A. Nakamura, K. Tanimura, and N. Itoh, Phys. Rev. Lett. **67**, 2701 (1991).

[13] K. Tanimura, T. Suzuki, and N. Itoh, Phys. Rev. Lett. **68**, 635 (1992).

[14] K. Kan'no, K. Tanaka, and T. Hayashi, Rev. Solid State Sci. **4**, 383 (1990).

[15] K. Tanimura and N. Itoh, Phys. Rev. B **45**, 1432 (1992).

[16] R. T. Williams, H. Liu, G. P. Williams, Jr., and K. J. Platt, Phys. Rev. Lett. **66**, 2140 (1991).

[17] K. Tanimura, N. Itoh, T. Hayashi, and H. Nishimura, J. Phys. Soc. Jpn. **61**, 1366 (1992).

[18] A. M. Stoneham, J. Phys. C **7**, 2476 (1974); K. S. Song, A. M. Stoneham, and A. H. Harker, *ibid.* **8**, 1125 (1976).

[19] M. N. Kabler, Phys. Rev. **136**, A1296 (1964).

[20] C. H. Leung and K. S. Song, J. Phys. C **12**, 3921 (1979).

[21] R. T. Williams, K. S. Song, W. L. Faust, and C. H. Leung, Phys. Rev. B **33**, 7232 (1986).

[22] K. S. Song and C. H. Leung, Rev. Solid State Sci. **4**, 357 (1990).

[23] K. S. Song, Rev. Solid State Sci. **5**, 477 (1991).

[24] R. C. Baetzold and K. S. Song, J. Phys. Condens. Matter **3**, 2499 (1991).

[25] A. L. Shluger, R. W. Grimes, and C. R. A. Catlow, J. Phys. Condens. Matter **3**, 3125 (1991).

[26] A. L. Shluger, N. Itoh, V. E. Puchin, and E. N. Heifets, Phys. Rev. B **44**, 1499 (1991).

[27] A. L. Schluger, N. Itoh, R. W. Grimes, and C. R. A. Catlow, Rev. Solid State Sci. **5**, 497 (1991).

[28] R. C. Baetzold and K. S. Song, Phys. Rev. B **46**, 1960 (1992).

[29] D. Pooley, Proc. Phys. Soc. London **81**, 245 (1966); **81**, 257 (1966).

[30] N. Itoh, A. M. Stonehma, and A. H. Harker, J. Phys. C **10**, 4197 (1977).

[31] C. J. Delbecq, J. L. Kilopus, E. L. Yasaitis, and P. H. Yuster, Phys. Rev. **154**, 866 (1967).

[32] R. T. Williams and M. N. Kabler, Phys. Rev. B **9**, 1897 (1974).

[33] G. B. Bachelet, D. R. Hamann, and M. Schluter, Phys. Rev. B **26**, 4199 (1982).

[34] See for review a special issue of J. Chem. Soc. Faraday Trans. II **85** (1989) edited by C. R. A. Catlow and A. M. Stoneham.

[35] M. J. Norgett (unpublished).

[36] A. M. Stoneham (unpublished).

[37] J. M. Vail, J. Phys. Chem. Solids **51**, 589 (1990).

[38] P. J. Hay and W. R. Wadt, J. Chem. Phys. **82**, 299 (1985).

[39] D. G. Bounds and A. Hinchliffe, Chem. Phys. Lett. **56**, 303 (1978).

[40] W. Kanzig and W. R. Woodruff, J. Phys. Chem. Solids **9**, 70 (1958).

[41] A. Ch. Lushchik, Yu. V. Kolk, N. E. Lushchik, and A. G. Fropir, Tr. Inst. Fiz. Astron. Akad. Nauk. Est. SSR Ser. Fiz. **58**, 7 (1986) (in Russian).

[42] T. Suzuki, K. Tanimura, N. Itoh, A. L. Shluger, and V. E. Puchin (unpublished).

[43] G. J. Dienes, R. D. Hatcher, and R. Smoluchowski, Phys. Rev. **157**, 692 (1967); E. A. Kotomin, A. L. Shluger, and Yu. R. Dzelwe, Phys. Status Solidi B **98**, 427 (1980).

[44] E. Goovarets and D. Schoemaker, Phys. Status Solidi B **88**, 615 (1978).

[45] P. E. Cade, A. M. Stoneham, and P. W. Tasker, Phys. Rev. B **30**, 4621 (1984).

[46] K. Tanimura (unpublished).

[47] R. Broer, A. B. Van Oosten, and W. C. Nieuwpoort, Rev. Solid State Sci. **5**, 70 (1991).

[48] L. I. Chen, K. S. Song, and C. H. Leung, Nucl. Instrum. Methods B **46**, 216 (1990).

[49] E. A. Vasil'chenko, N. E. Lushchik, and Ch. B. Lushchik, Fiz. Tverd. Tela (Leningrad) **12**, 211 (1970) [Sov. Phys. Solid State **12**, 167 (1970)].

[50] K. Tanimura and N. Itoh, J. Phys. Chem. Solids **42**, 901 (1981).

[51] N. Itoh, T. Eshita, and R. T. Williams, Phys. Rev. B **34**, 4230 (1986).

[52] S. Hirota, K. Edamatsu, and M. Hirai, Phys. Rev. Lett. **67**, 3283 (1991).

[53] K. Tanaka, K. Kan'no, and Y. Nakai, J. Phys. Soc. Jpn. **59**, 1474 (1990).

[54] R. T. Williams, H. Liu, G. P. Williams, Jr., and K. J. Platt, Phys. Rev. Lett. **66**, 2140 (1991).

[55] Y. Kayanuma, Rev. Solid State Sci. **4**, 403 (1990).